

Sox2

Biology and Role in Development and Disease

Edited by

HISATO KONDOH

Faculty of Life Sciences, Kyoto Sangyo University, Kyoto, Japan

ROBIN LOVELL-BADGE

The Crick Institute, London, UK



ELSEVIER

Amsterdam • Boston • Heidelberg • London

New York • Oxford • Paris • San Diego

San Francisco • Singapore • Sydney • Tokyo

Academic Press is an imprint of Elsevier



Academic Press is an imprint of Elsevier
125 London Wall, London EC2Y 5AS, UK
525 B Street, Suite 1800, San Diego, CA 92101-4495, USA
225 Wyman Street, Waltham, MA 02451, USA
The Boulevard, Langford Lane, Kidlington, Oxford OX5 1GB, UK

Copyright © 2016 Elsevier Inc. All rights reserved.

No part of this publication may be reproduced or transmitted in any form or by any means, electronic or mechanical, including photocopying, recording, or any information storage and retrieval system, without permission in writing from the publisher. Details on how to seek permission, further information about the Publisher's permissions policies and our arrangements with organizations such as the Copyright Clearance Center and the Copyright Licensing Agency, can be found at our website: www.elsevier.com/permissions.

This book and the individual contributions contained in it are protected under copyright by the Publisher (other than as may be noted herein).

Notices

Knowledge and best practice in this field are constantly changing. As new research and experience broaden our understanding, changes in research methods, professional practices, or medical treatment may become necessary.

Practitioners and researchers must always rely on their own experience and knowledge in evaluating and using any information, methods, compounds, or experiments described herein. In using such information or methods they should be mindful of their own safety and the safety of others, including parties for whom they have a professional responsibility.

To the fullest extent of the law, neither the Publisher nor the authors, contributors, or editors, assume any liability for any injury and/or damage to persons or property as a matter of products liability, negligence or otherwise, or from any use or operation of any methods, products, instructions, or ideas contained in the material herein.

British Library Cataloguing-in-Publication Data

A catalogue record for this book is available from the British Library

Library of Congress Cataloging-in-Publication Data

A catalog record for this book is available from the Library of Congress

ISBN: 978-0-12-800352-7

For information on all Academic Press publications
visit our website at <http://store.elsevier.com/>



Publisher: Shirley Decker-Lucke
Acquisition Editor: Shirley Decker-Lucke
Editorial Project Manager: Halima Williams
Production Project Manager: Julia Haynes
Designer: Matt Limbert

Typeset by TNQ Books and Journals
www.tnq.co.in

Printed and bound in the United States of America

CONTENTS

<i>List of Contributors</i>	<i>xi</i>
<i>Preface</i>	<i>xv</i>
Part 1: Basic Features of Sox2 Protein and Gene	1
1. Historical Perspectives	3
Hisato Kondoh and Robin Lovell-Badge	
Discovery of SOX2 and other SOX Genes Pioneered by Sry	3
SOX2 with Defined Regulatory Targets, in Cooperation with Partner Factors	5
Molecular Structure of SOX2 HMG and Associated Domains Interacting with DNA and Partner Factors	5
SOX2 Functions in the Early Developmental Process, Involving Functional Redundancy with SOXB1 Genes and Maternal Factors	6
Roles for SOX2 in Neural and Associated Tissues	7
SOX2 in the Development of Nonneural Tissues	7
SOX2 in the Stem Cells and a Potential New Role for SOX2 in Chromatin Regulation	8
Regulation of SOX2 Activity at Different Levels	9
SOX2 and Disease	9
References	10
2. Three-dimensional Structure of SOX Protein–DNA Complexes	15
Prasanna R. Kolatkar, Balasubramanian Moovarkumudalvan, Essam M. Abdelalim and Mohamed M. Emara	
Introduction	15
SOX HMG Domain Structure	16
Mechanism of Motif Recognition Facilitated by Structures	19
Structure-Assisted Re-Engineering of SOX Members	20
Conclusion	22
References	23
3. Dynamics of SOX2 Interactions with DNA	25
G. Marius Clore	
Introduction	25
Experimental Approaches	26
Interactions of SOX2 with Nonspecific DNA	29
Kinetics of Intermolecular Translocation of SOX2 between Specific DNA Duplexes	32
Interplay between SOX2 and Oct1 in Translocation Involving Sparsely Populated States Probed by PRE	36

Concluding Remarks	39
Acknowledgments	40
References	40
4. Posttranscriptional Modulation of Sox2 Activity by miRNAs	43
Nilima Prakash	
Introduction	43
Biogenesis and Function of microRNAs and Large Intergenic Noncoding RNAs in Animals	44
Modulatory Roles of microRNAs in the Posttranscriptional Control of Gene Expression	47
ncRNA-Mediated Modulation of SOX2 Expression in PSCs	48
miRNA-Mediated Modulation of SOX2 Expression in Neural Stem/Progenitor Cells	55
miRNA-Mediated Modulation of SOX2 Expression in CSCs	58
Keeping SOX2 Activity in Check: Some Concluding Remarks on Posttranscriptional Modulation of SOX2 Expression	63
Acknowledgments	65
References	65
5. The Role of SOX2-Interacting Proteins in Gene Regulation by SOX2	73
Raymond A. Poot	
Introduction	73
Unbiased Identification of SOX2 Interaction Partners	74
SOX2 in ESCs	75
SOX2 in TSCs	78
SOX2 in NSCs	78
Eye	81
Concluding Remarks	82
References	83
Part 2: Gene Regulatory Networks Centered by Sox2	87
6. Evolution of Sox2 and Functional Redundancy in Relation to Other SoxB1 Genes	89
Yusuke Kamachi	
Introduction	89
The Sox Family and HMG Domain Superfamily	89
Evolution of the SOX Family Genes	93
Expansion of the SOX Genes and Emergence of SOX2 in the Vertebrate Lineage	95
Functional Redundancy and Diversification among the SOXB1 Genes	98
Diversification of SOXB into SOXB1 and SOXB2 through Tandem Duplication	100
Evolutionary Pathway of SOXB Genes	101
References	103

7. Regulation of Sox2 via Many Enhancers of Distinct Specificities	107
Masanori Uchikawa and Hisato Kondoh	
Introduction	107
Characterization of Neural Enhancers Distributed in the 50-kb Sox2-Proximal Region of the Chicken Genome	109
Characterization of Individual Enhancers that Exhibit Activities in the Neural Primordia	110
Additional Enhancers Outside the Central 50-kb Region	118
Hierarchy in the Action of Sensory Placode-Specific Enhancers	121
Correlations between the Enhancers and the Conserved Sequence Blocks	122
Comparison with Sox3 Enhancers	123
Relationships among SOX2-Associated Enhancers, Conserved Sequence Blocks, and Sox2ot Exons	124
Conclusions	126
References	126
8. SOX2–Partner Factor Interactions and Enhancer Regulation	131
Hisato Kondoh and Yusuke Kamachi	
Introduction	131
SOX2–POU5F1 Interaction	131
Cases for Overlap of High-Density Clusters of SOX2 Binding and POU Binding Sequences	135
SOX2–PAX6 Interaction	137
SOX2-Interacting Chromatin Modification Factors and Covalent Modification of the SOX2 Protein	139
Other Cases of Gene Regulation That Depend on SOX2–Partner Factor Interaction	141
References	142
9. Genomic Occupancy in Various Cellular Contexts and Potential Pioneer Factor Function of SOX2	145
Jonas Muhr	
Introduction	145
SOX2 Function and Binding Pattern in Pluripotent Stem Cells	145
Prebinding of Lineage-Specific Genes in Pluripotent Stem Cells	148
SOX2 Function in Tissue-Specific Stem Cells	148
SOX2 Binding Pattern in Stem and Progenitor Cells of the Developing CNS	149
Specification of SOX2 Binding	151
Functions of Genes Bound by SOXB1 Proteins in NPCs	152
Prebinding of Neuronal Genes by SOXB1 Proteins in NPC	153
Pioneering Activity of SOX2 During Cellular Reprogramming	154
Concluding Remarks	156
References	157

Part 3: Sox2 Regulatory Functions in Specific Cells and Tissues	161
10. SOX2-Dependent Regulation of Pluripotent Stem Cells	163
Frederick C.K. Wong, Ian Chambers and Nicholas P. Mullin	
Introduction	163
SOX2–Protein Partner Interactions	164
Regulation of Sox2	170
Consequences of Altering SOX2 Levels	172
SOX2 in Reprogramming	177
SOX2 in Epiblast Stem Cells	178
Perspectives	179
Acknowledgments	180
References	180
11. SOX2-Dependent Regulation of Neural Stem Cells and CNS Development	187
Jessica Bertolini, Sara Mercurio, Rebecca Favaro, Jessica Mariani, Sergio Ottolenghi and Silvia K. Nicolis	
Introduction	187
SOX2 Expression Marks the Developing CNS	187
Transcriptional Regulation of Sox2 Expression in Neural Cells	189
SOX2 Functions and Molecular Targets in CNS Development	195
SOX2 Functions in NSC In Vitro	204
SOX2 Targets in NSC	205
Open Questions and Perspectives	210
References	212
12. Multiple Roles for SOX2 in Eye Development	217
Hisato Kondoh, Masanori Uchikawa and Yasuo Ishii	
Introduction	217
Steps Involved in Embryonic Eye Development	217
Expression of Sox2 in Eye Tissues and Its Regulation	220
Enhancers That Regulate Sox2 Expression during Eye Development	220
Taxon-Dependent Expression of SOXB1 Factors and Unique Contribution of SOX2 in Mammalian Eye Development	222
Roles for SOX2 at Distinct Stages of Retinal Development	223
Roles for SOX2 in Regulating RPC Maintenance Involving Notch1 Activation and in the Cell Identity of Ganglion Cells, a Subset of Amacrine Cells, and Müller Cells	225
Cooperation of SOX2 and PAX6 in Lens Development	226
Mechanisms Underlying Lens Transdifferentiation and Lens Regeneration	228
References	230

13. Congenital Abnormalities and SOX2 Mutations	235
Veronica van Heyningen	
Identification of <i>SOX2</i> as a Key Gene Mutated in Bilateral Anophthalmia and Severe Microphthalmia Cases	235
Deciphering the Role of <i>SOX2</i> in Development and Disease	236
The Spectrum of <i>SOX2</i> Mutations in Ocular Malformation and Related Anomalies	238
Limited Genotype–Phenotype Correlations	239
References	240
14. Role of SOX2 in the Hypothalamo–Pituitary Axis	243
Karine Rizzoti and Robin Lovell-Badge	
Introduction	243
Expression of <i>SOX2</i> in the Hypothalamo–Pituitary Axis	245
Role of <i>SOX2</i> in Hypothalamo–Pituitary Axis Morphogenesis	248
<i>SOX2</i> in the Postnatal Axis	253
<i>SOX2</i> and Human Disorders Affecting the Hypothalamo–Pituitary Axis	256
Conclusion	258
References	258
15. SOX2 in Neurosensory Fate Determination and Differentiation in the Inner Ear	263
Kathryn S.E. Cheah and Pin-Xian Xu	
Inner Ear Development	263
<i>SOX2</i> Expression in the Developing Inner Ear	264
<i>SOX2</i> is Essential for Prosensory Specification in Early Otic Development	267
Widely Separated Deoxyribonucleic Acid Enhancers Direct Otic <i>SOX2</i> Expression	267
<i>SOX2</i> and Inner Ear Neurogenesis	268
<i>SOX2</i> and Sensory Cell Fate Specification and Differentiation in the Cochlear Epithelium	269
The <i>SOX2</i> Gene Regulatory Network: Cooperation with Signaling Pathways and Partners	270
<i>SOX2</i> in Hair Cell Fate Induction in Concert with Partners	271
Perspective and Regenerative Medicine for the Inner Ear	275
Acknowledgments	276
References	276
16. SOX2 in the Skin	281
Natacha A. Agabalyan, Andrew Hagner, Waleed Rahmani and Jeff Biernaskie	
Sox2 Expression in the Epidermis	282
Sox2 Expression in the Hair Follicle	284
<i>SOX2</i> Expression in Skin Cancers and Wounds	291

Conclusion	296
References	297
17. SOX2 in the Development and Maintenance of the Trachea, Lung, and Esophagus	301
Neng Chun Wong, Parth Armin, Ming Jiang, Wei-Yao Ku, Ian Jacobs and Jianwen Que	
Introduction	301
SOX2 in Separation of the Trachea and Esophagus	302
SOX2 in Lung Development and Maintenance	304
SOX2 in Morphogenesis and Maintenance of Esophagus	312
Conclusion Remarks and Future Direction	314
Acknowledgments	315
References	316
<i>Index</i>	321

PREFACE

Sox2, which collectively refers to the *Sox2* gene and its encoded transcription factor SOX2, has a remarkable research history over a quarter of a century that marks the progress in our understanding of transcriptional regulation in higher organisms. The central importance of Sox2 in various biological processes such as embryogenesis, organogenesis, stem cell regulation, and diseases has also gained increasing attention. We thought it was timely to compile and organize our current knowledge on Sox2 in the form of a book, with comprehensive coverage from its molecular nature to organismal regulation. Thanks to the many specialists from various branches of Sox2 research who approved our idea and contributed chapters, we believe that our undertaking was successful. We hope that this book will become a useful resource for biomedical scientists of various disciplines, from students to professionals.

We missed one potential author who should have contributed to this book, the late Larysa Pevny, who passed away in 2012 at the age of just 47 years. She made important contributions to the study of Sox2, as you will see in many citations in various chapters. She also shared valuable mouse models produced by her with many laboratories around the world, which promoted Sox2 research. On this occasion, we would like to mention these contributions in tribute to her.

We once again thank the authors for their professional contributions, and Dr Jianwen Que and Dr Masanori Uchikawa for providing the beautiful figure panels for the front cover: immunostained embryonic trachea and lung (bottom left; see Chapter 17 Figure 3 for details) and enhanced green fluorescent protein fluorescence of a *Sox2-IRES-EGFP* knock-in E9 mouse embryo (bottom right). We also appreciate the patience and expert management of the editorial team of Academic Press/Elsevier, particularly Halima N. Williams, Elizabeth Gibson, and Julia Haynes, who made this undertaking possible.

Hisato Kondoh and Robin Lovell-Badge

CHAPTER 3

Dynamics of SOX2 Interactions with DNA

G. Marius Clore

Laboratory of Chemical Physics, National Institute of Diabetes and Digestive and Kidney Diseases, National Institutes of Health, Bethesda, MD, USA

INTRODUCTION

Sox proteins are members of the HMG-box family of architectural factors that bind to the minor groove of deoxyribonucleic acid (DNA), bending the DNA by 50–90° (Kamachi et al., 2000; Dailey and Basilico, 2001; Murphy et al., 2001) (see also Chapter 2). The Sox proteins generally act as part of various multitranscription factor complexes, thereby integrating a wide array of signaling pathways by way of combinatorial transcriptional control to provide temporal and cell-specific transcription regulation (Wolberger, 1999). An example of this phenomenon is provided by members of the Sox and Oct transcription factor families that interact with a variety of DNA promoter/enhancer elements to regulate transcription during embryogenesis and neural development (Kamachi et al., 2000; Dailey and Basilico, 2001) (see also Chapters 5 and 8).

Ternary complexes of SOX2 and OCT1 bound to the regulatory elements within the *HOXB1* promoter and fibroblast growth factor-4 (*FGF4*) enhancer have been solved by nuclear magnetic resonance (NMR) spectroscopy (Williams et al., 2004) and X-ray crystallography (Remenyi et al., 2003), respectively. The two promoters differ in the spacing between the SOX2 and OCT1 binding sites, thereby altering the relative orientations of the two proteins and the protein–protein interface in the two complexes (Figure 1). In the case of the *HOXB1* promoter, the SOX2 and OCT1 sites are immediately adjacent to one another, whereas they are separated by three base pairs on the *FGF4*-enhancer. As a result, the protein–protein interface is approximately double in size for the former ternary complex relative to the latter (Williams et al., 2004).

In this brief review, I will summarize our work on the dynamics of SOX2–DNA interactions in the context of specific and nonspecific SOX2–DNA complexes and specific SOX2–OCT1–DNA ternary complexes involving both *HOXB1* and *FGF4* DNA (Takayama and Clore, 2012a,b). These studies involve the application of NMR spectroscopy—in particular, three major techniques: line-shape analysis, *z*-exchange spectroscopy, and paramagnetic relaxation enhancement (PRE) spectroscopy—which will be briefly described in the next section. Using these methods, we are able to directly probe the mechanisms whereby these two transcription factors locate their

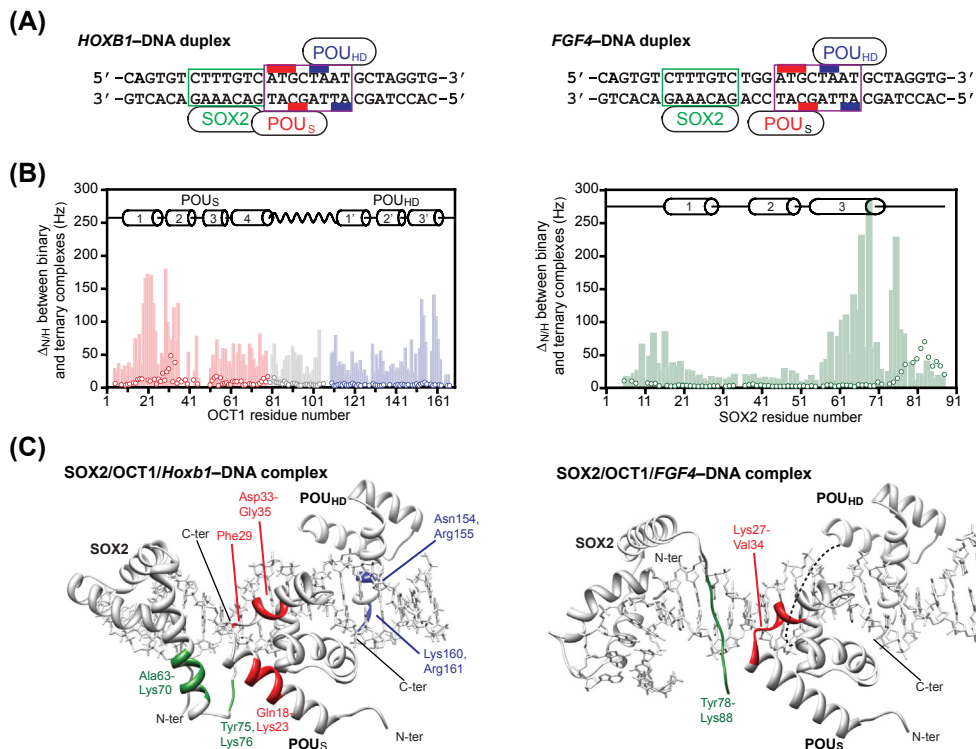


Figure 1 Structures of the ternary SOX2-OCT1-DNA complexes on the *HOXB1* promoter and *FGF4* enhancer. (A) Sequences of the *HOXB1* and *FGF4*-like DNA duplexes. The latter does not represent the actual *FGF4* enhancer sequence but adds the 3-bp insertion (TTG) between the specific binding sites for SOX2 and OCT1, thereby ensuring that differences in binding and kinetics observed for these two sequences solely reflect the 3-bp insertion. (B) $^1\text{H}_\text{N}/^{15}\text{N}$ backbone chemical shift perturbation mapping of OCT1 (left) and SOX2 (right) upon ternary complex formation on *HOXB1* (light bars) and *FGF4* (open circles) DNA. (C) Three-dimensional structures of the SOX2-OCT1-*Hoxb1*-DNA (PDB 1o4x) and SOX2-DNA *Fgf4*-DNA (PDB 1gt0) complexes determined by NMR (Williams et al., 2004) and X-ray crystallography (Remenyi et al., 2003), respectively. Residues showing significant $^1\text{H}_\text{N}/^{15}\text{N}$ chemical shift perturbations (>100 Hz for the SOX2-OCT1-*Hoxb1*-DNA complex and >20 Hz for the SOX2-OCT1-*Fgf4*-DNA complex) are mapped onto the structures. Adapted from Takayama and Clore (2012a).

specific target sites on the DNA within an overwhelming sea of nonspecific DNA and to study the effect of protein-protein interactions on global intermolecular translocation rates.

EXPERIMENTAL APPROACHES

The primary experimental approach we employed to study the dynamics of SOX2-DNA interactions involves the application of three NMR techniques: line-shape analysis, $^{15}\text{N}_z$ -exchange spectroscopy, and PRE.

Exchange Kinetics

The strategy we developed to study the kinetics of intermolecular exchange of a transcription factor between two different DNA molecules (with or without the specific target site present) involves a simple strategy in which the sequences of two DNA molecules, A and B, are slightly different (Iwahara and Clore, 2006b; Iwahara et al., 2006). The difference may involve one or two bases at the edge of a specific target site when considering specific protein–DNA interactions, or randomly within a restricted region covering the length of a binding site (say, six to eight bases) when considering nonspecific protein–DNA interactions. The result is that the backbone chemical shifts ($^1\text{H}_\text{N}$ and ^{15}N) for the uniformly ^{15}N -labeled transcription factor will be slightly different when bound to either DNA-A or DNA-B.

When intermolecular exchange of the transcription factor between the two DNA molecules is slow (defined as $k_{\text{ex}} \ll 2\pi\Delta\nu$, where $\Delta\nu$ is the difference in Hz between the chemical shifts of the two states), two sets of resonances will be observed corresponding to the two complexes with the different DNA molecules, and the rate constants for the exchange process can be readily determined by fitting the mixing time dependence of the magnetization of auto- ($M_z^{AA}; M_z^{BB}$) and exchange cross- ($M_z^{AB}; M_z^{BA}$) peaks in a two-dimensional $^{15}\text{N}_z$ -exchange spectrum given by a matrix form of the McConnell equations (McConnell, 1958):

$$\frac{d}{dT_{\text{mix}}} \begin{pmatrix} M_z^{AA} \\ M_z^{BB} \\ M_z^{AB} \\ M_z^{BA} \end{pmatrix} = - \begin{bmatrix} (k_{AB}^{\text{app}} + R_1^A) & 0 & -k_{BA}^{\text{app}} & 0 \\ 0 & (k_{BA}^{\text{app}} + R_1^B) & 0 & -k_{AB}^{\text{app}} \\ -k_{AB}^{\text{app}} & 0 & (k_{BA}^{\text{app}} + R_1^B) & 0 \\ 0 & -k_{BA}^{\text{app}} & 0 & (k_{AB}^{\text{app}} + R_1^A) \end{bmatrix} \begin{pmatrix} M_z^{AA} \\ M_z^{BB} \\ M_z^{AB} \\ M_z^{BA} \end{pmatrix} \quad (1)$$

where k_{AB}^{app} and k_{BA}^{app} are the apparent rate constants for transfer of the transcription factor from DNA-A to DNA-B and vice versa, respectively, and R_1^A and R_1^B are the longitudinal relaxation rates of the protein in complex with DNA-A and DNA-B, respectively.

When exchange of the transcription factor between the two DNA molecules is intermediate ($k_{\text{ex}} \sim 2\pi\Delta\nu$) or fast ($k_{\text{ex}} \ll 2\pi\Delta\nu$), only a single cross-peak per residue will be observed in the ^1H - ^{15}N correlation spectrum of the protein. Under these conditions, the $^1\text{H}_\text{N}$ transverse relaxation rate for a given protein residue, either measured directly in the ^1H dimension from the spectrum (using Lorentzian line-shape fitting) or through transverse (R_2) relaxation measurements, is related to the rate of exchange (k_{ex}) of the transcription factor between DNA-A and DNA-B. The observed transverse relaxation rate R_2^{obs} is given by:

$$R_2^{\text{obs}} = p_A R_2^A + p_B R_2^B + R_{\text{ex}}^{\text{inter}} \quad (2)$$

where p_A and p_B are the populations of the transcription factor bound to DNA-A and DNA-B, respectively; R_2^A and R_2^B are the corresponding R_2 rates for the protein in states A and B; and $R_{\text{ex}}^{\text{inter}}$ is the exchange contribution arising from intermolecular translocation of the transcription factor between DNA-A and DNA-B. In the intermediate exchange regime, R_2^{obs} can only be calculated numerically using the McConnell equations (McConnell, 1958), but in the fast exchange regime $R_{\text{ex}}^{\text{inter}}$ can be calculated analytically using the equation (Iwahara et al., 2006):

$$R_{\text{ex}}^{\text{inter}} = 4\pi^2 \Delta \nu^2 p_A p_B / k_{\text{ex}}^{\text{inter}} \quad (3)$$

where

$$k_{\text{ex}}^{\text{inter}} = k_{\text{AB}}^{\text{app}} + k_{\text{BA}}^{\text{app}}$$

Intermolecular translocation of a transcription factor between two DNA duplexes can occur via two mechanisms that are readily dissected by examining the dependence of the apparent exchange rate constants on the concentration of free DNA (Iwahara and Clore, 2006b; Iwahara et al., 2006; Doucleff and Clore, 2008): (1) Spontaneous dissociation of the protein into free solution followed by reassociation of free protein and DNA is a first-order process that is independent of DNA concentration (under conditions where the total DNA is in excess over protein and the dissociation rate constant is significantly smaller than the pseudo-first-order association rate constant); and (2) direct intermolecular transfer from one DNA duplex to another without dissociation of the protein into free solution is a bimolecular exchange reaction whose rate is directly proportional to the concentration of free DNA. Thus, the slope of a plot of the apparent first-order rate constants versus the concentration of free DNA yields the bimolecular rate constants for direct intermolecular transfer, whereas the intercept is equal to half the dissociation rate constant (the statistical factor of 2 arising from transitions between the same species).

PRE and Detection of Short-Lived Binding Intermediates

The PRE arises from magnetic dipolar interactions between a nucleus (usual protons) and the unpaired electrons of a paramagnetic center and results in an increase in the rate of nuclear magnetization, generally measured as the transverse PRE, Γ_2 , given by the difference in R_2 rates between the paramagnetic sample and a diamagnetic control (Clore and Iwahara, 2009). In studying protein-DNA complexes, the simplest strategy involves introducing (d)T-ethylenediaminetetraacetic acid (EDTA) chelated, for example, to Mn^{2+} for the paramagnetic sample and Ca^{2+} for the diamagnetic control, at a particular site synthetically, and measuring the intermolecular PRE effects on a uniformly ^{15}N -labeled protein using ^1H - ^{15}N correlation-based experiments (Iwahara et al., 2003; Iwahara and Clore, 2006a). The magnitude of the PRE effect is proportional to the

inverse sixth power of the ensemble average of the distance r between the nucleus of interest and the paramagnetic center. Because of the large magnetic moment of the unpaired electron, these effects can extend out to sizable distances (up to about 35 Å for Mn^{2+}). When exchange between a major species and an invisible minor species is slow on the PRE time scale, the observed Γ_2 values will simply reflect the Γ_2 values for the major species. However, when the exchange between these species is fast, the observed Γ_2 values will be population-weighted averages of the Γ_2 values for the major and minor species (Iwahara and Clore, 2006a; Clore and Iwahara, 2009). If there are distances between the paramagnetic label and several protons that are significantly shorter in the minor species than the major one, the footprint of the minor species will be apparent in the PRE profiles measured on the major species, even though the minor species may constitute less than 1% of the total population. These effects can be used to directly probe the involvement of sparsely populated states in the search process whereby transcription factors locate their specific target site within an overwhelming sea of nonspecific DNA sites by measuring the intermolecular PRE profiles observed on the transcription factor in the presence of DNA paramagnetically tagged (usually dT-EDTA- Mn^{2+}) at several locations (one at a time) (Iwahara and Clore, 2006a; Clore, 2011a,b; Takayama and Clore, 2011).

Dissecting the contributions to the intermolecular PREs from intramolecular sliding of the protein along the DNA and intermolecular translocation between DNA molecules can be accomplished by carrying out experiments in the presence of an equimixture of specific and nonspecific DNA (Iwahara and Clore, 2006a; Takayama and Clore, 2011, 2012b). In one sample, the nonspecific duplex is paramagnetically tagged so that intermolecular PREs can only occur via intermolecular translocation between the DNA bearing the specific site (whose spectrum is observed) and the paramagnetically tagged nonspecific DNA. In the second sample, the specific DNA is paramagnetically tagged and the observed PREs will therefore have contributions from both intra- and intermolecular translocation. If sliding (intramolecular translocation) and intermolecular translocation occur, the ratio of the PREs of sample 2 to sample 1 will be larger than 1.

INTERACTIONS OF SOX2 WITH NONSPECIFIC DNA

Sampling of Nonspecific DNA by SOX2

Intermolecular PRE profiles were measured for ^{15}N -labeled SOX2 in the presence of a 29-base pair (bp) DNA duplex with the (d)T-EDTA- Mn^{2+} paramagnetic label covalently attached to a thymine base at either end (Figure 2(A)) (Takayama and Clore, 2012b). Because the exchange of SOX2 between nonspecific sites is fast, the PRE profiles are a weighted average over all possible nonspecific configurations. The PRE profiles arising from the paramagnetic label at the two sites are similar both qualitatively and quantitatively (Figure 2(B) and (C)). The regions of SOX2 that exhibit significant PREs

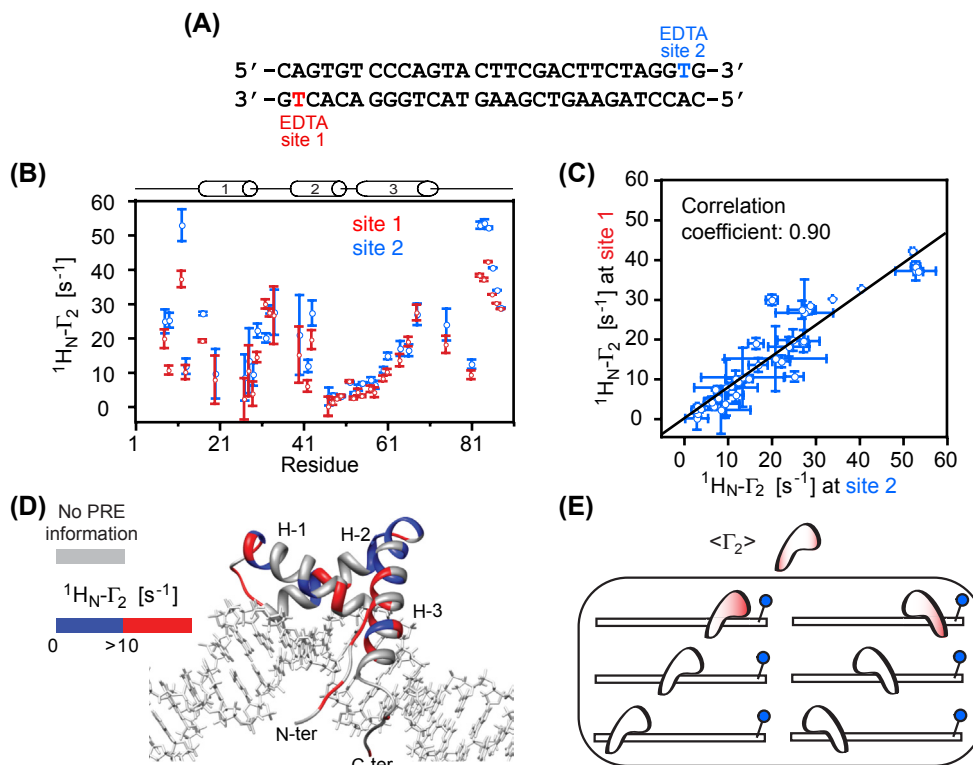


Figure 2 Sampling of binding sites upon nonspecific binding of SOX2 to DNA. (A) Sequence of nonspecific DNA duplex used for PRE measurements. The paramagnetic label (EDTA chelated to Mn^{2+}) was added to two thymines individually (red, site 1; blue, site 2) located at the two ends of the duplex. (B) PRE profiles measured on backbone amide protons ($^1\text{H}_\text{N}-\Gamma_2$) from sites 1 and 2. (C) Correlation between PREs observed from sites 1 and 2. (D) PRE profiles originating from site 2 mapped onto the structure of the specific SOX2-DNA complex (color scale shown on left). (E) Schematic representation of nonspecific DNA binding states sampled by SOX2 (with SOX2 in two orientations related by 180° rotation relative to the long axis of the DNA) with color coding representing the strength of the PRE and the paramagnetic label depicted by the blue sphere. Adapted from [Takayama and Clore \(2012b\)](#).

($^1\text{H}-\Gamma_2 > 10 \text{ s}^{-1}$) are all located in structural elements that are in close proximity to the DNA ([Figure 2\(D\)](#)). One can therefore conclude that SOX2 binds to numerous nonspecific binding sites in two orientations, related by 180° rotation relative to the long axis of the DNA ([Figure 2\(E\)](#)). These results are similar to those observed for the sampling of nonspecific DNA binding sites by the related HMG-box family member HMG-B1, which only binds nonspecifically to DNA ([Iwahara et al., 2004](#)).

Kinetics of Intermolecular and Intramolecular Translocation of SOX2 on Nonspecific DNA

To examine the rates of intermolecular and intramolecular translocation of SOX2 on nonspecific DNA, we measured R_2 rates (using line-width analysis) for complexes of SOX2 with two different nonspecific DNA duplexes (Figure 3(A)), both individually and as 1:1 mixtures, as a function of DNA concentration (Takayama and Clore, 2012b). Several resonances exhibit significant $^1\text{H}_\text{N}$ or ^{15}N chemical shift differences between the two nonspecific complexes, and the corresponding cross-peaks in the sample comprising a 1:1 mixture of the nonspecific complexes appear halfway between those for the individual complexes and are broadened owing to the exchange contribution from intermolecular translocation (Figure 3(B)). The R_2 rates for the individual complexes are

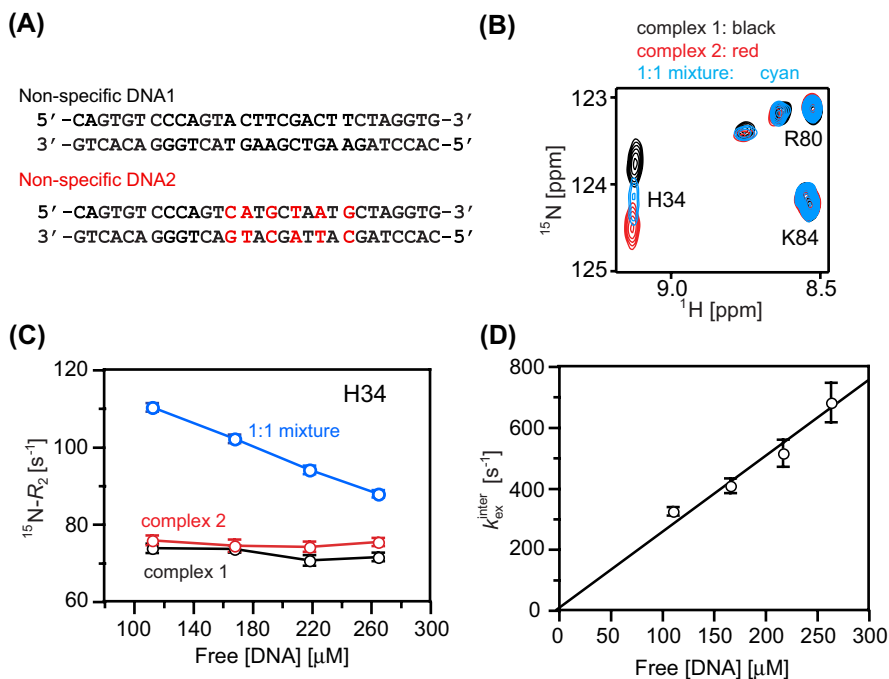


Figure 3 Intermolecular translocation of SOX2 between nonspecific DNA duplexes studied by line-width analysis. (A) Sequences of the two nonspecific DNA duplexes used with the base changes between the two duplexes indicated in red in the second DNA duplex. (B) Selected region of the ^1H - ^{15}N correlation spectra of $^{15}\text{N}/^2\text{H}$ -labeled SOX2 for complexes with the first (black) and second (red) DNA duplexes, and a 1:1 mixture of both DNA duplexes (cyan) at 30 °C in the presence of 25 mM added NaCl. The concentration of SOX2 is 0.4 mM; the concentration of duplexes is 0.5 mM in the individual complexes and 0.25 mM in the 1:1 mixture of the two complexes. (C) Dependence of transverse relaxation rates as a function of free DNA concentration. (D) Dependence of the overall apparent intermolecular translocation rate, $k_{\text{ex}}^{\text{inter}}$, on the free DNA concentration. Adapted from Takayama and Clore (2012b).

unaffected by the concentration of free DNA, but those for the 1:1 mixture decrease as the concentration of DNA increases (Figure 3(C)). The apparent intermolecular rate constant, $k_{\text{ex}}^{\text{inter}}$, calculated from Eqn (3), is linearly proportional to the free DNA concentration (Figure 3(D)), indicative of direct transfer from one DNA duplex to the other without dissociation of SOX2 into free solution, and yields a second-order association rate constant of about $10^6 \text{ M}^{-1} \text{ s}^{-1}$.

The R_2 rates for the individual complexes are independent of DNA concentration (Figure 3(C)). Because these R_2 rates include an exchange contribution from intramolecular translocation (i.e., sliding) and because one can assume that the average chemical shift difference between nonspecific sites on a single DNA molecule will be approximately the same as those between the complexes with the two different nonspecific DNA duplexes, one can conclude that the rate for intramolecular translocation, $k_{\text{ex}}^{\text{intra}}$, is much faster than that for intermolecular translocation (Iwahara et al., 2006), which allows one to obtain a lower limit for $k_{\text{ex}}^{\text{intra}}$ from the extrapolated value of $k_{\text{ex}}^{\text{inter}} \sim 900 \text{ s}^{-1}$ at the free DNA concentration (about $360 \mu\text{M}$) when the R_2 rates for the 1:1 mixture are the same as those for the individual complexes (Figure 3(C) and (D)). This corresponds to a lower limit of about $0.1 \mu\text{m}^2 \text{ s}^{-1}$ for the one-dimensional diffusion coefficient for sliding (Clore, 2011b).

KINETICS OF INTERMOLECULAR TRANSLOCATION OF SOX2 BETWEEN SPECIFIC DNA DUPLEXES

The Binary SOX2 DNA Complex

The rates for intermolecular translocation of SOX2 between the two specific sites, differing by a single bp mutation just 5' of the 7-bp recognition sequence (Figure 4(A) and (B)), can be readily determined from $^{15}\text{N}_z$ -exchange experiments by monitoring the auto- and exchange-peak intensities in a ^1H - ^{15}N TROSY-based z -exchange spectrum (Sahu et al., 2007) (Figure 4(C) and (D)) as a function of mixing time for those residues that exhibit significantly different $^1\text{H}_\text{N}/^{15}\text{N}$ chemical shifts in the two complexes (Takayama and Clore, 2012b). In contrast to nonspecific binding in which the exchange of SOX2 between the two different nonspecific DNA duplexes was fast on the chemical shift time scale, exchange between the specific complexes is slow owing to tight binding (K_D about 10 nM at 150 mM NaCl) so that there are two sets of cross-peaks, one for each complex. Also in contrast to the nonspecific case, the apparent intermolecular exchange rate constants, $k_{\text{AB}}^{\text{app}}$ and $k_{\text{BA}}^{\text{app}}$, are independent of the concentration of free DNA (Figure 4(E)), which indicates that dissociation from the DNA is rate-limiting and intermolecular transfer occurs exclusively via full dissociation followed by reassociation (Takayama and Clore, 2012b). The dissociation rate constants given by $k_{\text{A}}^{\text{off}} = 2k_{\text{AB}}^{\text{app}}$ and $k_{\text{B}}^{\text{off}} = 2k_{\text{BA}}^{\text{app}}$ have values of $5\text{--}6 \text{ s}^{-1}$ at 30°C , from which one can calculate corresponding association rate constants (given the measured K_D of about 10 nM) of approximately

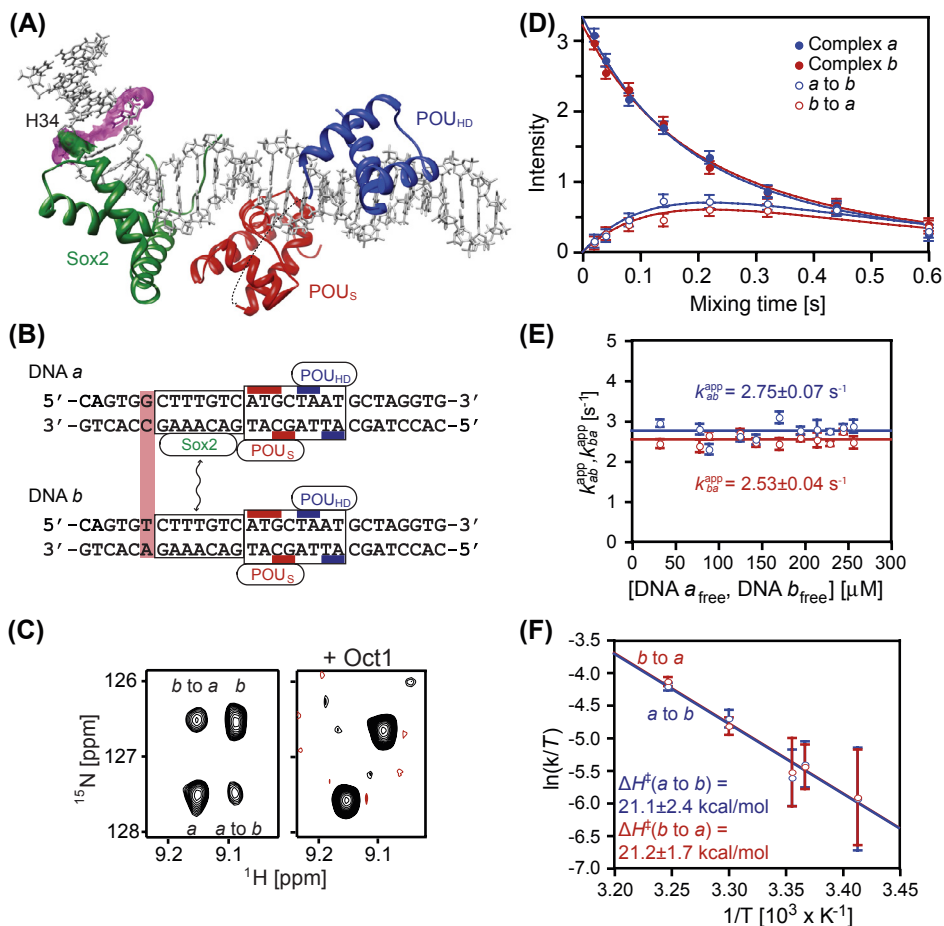


Figure 4 Intermolecular translocation of SOX2 between specific DNA complexes studied by ¹⁵N₂-exchange spectroscopy. (A) Structure of the SOX2-OCT1-*Hoxb1*-DNA complex with SOX2 in green and the POU_S and POU_{HD} domains of OCT1 in red and blue, respectively. (B) Sequences of the two DNA duplexes used for the ¹⁵N₂-exchange experiments with the bp difference between the two duplexes indicated by the purple bar (and also shown in purple in panel A). (C) Example of ¹⁵N₂-exchange data at a mixing time of 120 ms showing auto (*a* and *b*) and exchange (*a* to *b*, and *b* to *a*) peaks. Exchange is abolished upon addition of OCT1 (right panel). (D) Mixing time dependence of auto- and exchange peaks. (E) The apparent intermolecular exchange rates are independent of the concentration of free DNA, indicating that intermolecular exchange proceeds via dissociation followed by reassociation. (F) Eyring plots of the apparent intermolecular exchange rates as a function of temperature. Adapted from Takayama and Clore (2012b).

$5 \times 10^8 \text{ M}^{-1} \text{ s}^{-1}$. The temperature dependence of the dissociation rate constants (Figure 4(F)) yields values of ~ 21 and $\sim 4 \text{ kcal} \cdot \text{mol}^{-1}$ for the activation enthalpy (ΔH^\ddagger) and entropy ($T\Delta S^\ddagger$), respectively, indicating that the energy barrier to dissociation is largely enthalpic.

The Ternary SOX2-CT1-*Hoxb1*-DNA Complex

In the *HOXB1* promoter, the specific DNA binding sites for SOX2 and OCT1 are immediately adjacent to one another, burying about 540 \AA^2 of accessible surface at the interface between SOX2 and the POU_S domain of OCT1 (Williams et al., 2004) (cf. Figure 1 (C), left panel). Upon addition of OCT1, the rates of intermolecular translocation of both SOX2 and OCT1 are dramatically reduced and no longer detectable by *z*-exchange spectroscopy (Douceff and Clore, 2008; Takayama and Clore, 2012b) (cf. Figure 4(C), right panel where no exchange peaks are observed for SOX2 upon addition of OCT1). Given a ^{15}N - R_1 relaxation rate of about 1 s^{-1} , the minimum exchange rate measurable by $^{15}\text{N}_z$ -exchange spectroscopy is about 0.2 s^{-1} , so that the intermolecular exchange rates for both SOX2 and OCT1 between specific sites in the context of the ternary complex on the *HOXB1* promoter are reduced by at least an order of magnitude relative to those in the binary complexes.

The Ternary SOX2-OCT1-*Fgf4*-DNA Complex

In the *FGF-4* enhancer, the specific binding sites for SOX2 and OCT1 are separated by 3bp, and only about 240 \AA^2 of accessible surface is buried at the interface between SOX2 and OCT1 (Remenyi et al., 2003) (Figure 1(C), right panel). As a result, the reduction in intermolecular exchange rate constants is significantly less than that in the ternary complex on the *HOXB1* promoter, enabling one to probe the impact of protein-protein interactions on global exchange rates using $^{15}\text{N}_z$ -exchange spectroscopy and on cooperative binding using equilibrium fluorescence anisotropy measurements (Takayama and Clore, 2012a).

The K_D s values for the binding of SOX2 and OCT1 to their respective sites on the *FGF-4* enhancer are 5.3 and 44 nM, respectively. These are reduced by about 16-fold (to approximately 0.33 and 2.7 nM) in the context of the ternary complex (Takayama and Clore, 2012a).

The association and dissociation rate constants for the binding of SOX2 are increased (from about 1×10^9 to about $5 \times 10^9 \text{ M}^{-1} \text{ s}^{-1}$) and decreased (from about 5.3 to 1.5 s^{-1}), respectively, in the presence of OCT1. As in the case of the binary SOX2-DNA complex, the intermolecular transfer of SOX2 occurs by jumping (i.e., dissociation and reassociation) and does not involve direct intermolecular transfer (Takayama and Clore, 2012a). For OCT1, however, both jumping and direct intermolecular transfer mechanisms are operative (Takayama and Clore, 2012a). In the presence of SOX2, the dissociation rate constant for OCT1 is reduced by about 20% (from 4.4 to 3.5 s^{-1}), whereas the association rate constant is increased by over 10-fold (from approximately 1×10^8 to $13 \times 10^8 \text{ M}^{-1} \text{ s}^{-1}$). The direct intersegment transfer rate constant for the POU_{HD} domain is unaffected by the presence of SOX2 (about $1.8 \times 10^4 \text{ M}^{-1} \text{ s}^{-1}$) but that for the POU_S domain is reduced by close to 40% (from 3.4×10^4 to $2.2 \times 10^4 \text{ M}^{-1} \text{ s}^{-1}$), which is expected because SOX2 only contacts POU_S in the ternary complex.

These data lead us to propose the following model for the sequence of binding, intersegment transfer, and dissociation events involved in the combinatorial control of

gene expression by SOX2 and OCT1 (Takayama and Clore, 2012a) (Figure 5). The initial step involves binding of SOX2 to its specific DNA target site, as supported by the observation that the association rate constant for the formation of the SOX2:DNA binary complex is 10-fold higher than that for OCT1 and that the intermolecular translocation rate for SOX2 is slow, involving full dissociation, whereas that for OCT1 is rapid owing to direct intermolecular transfer at high DNA concentrations. This is also consistent with the localization of SOX2 to the cell nucleus, whereas OCT1 is

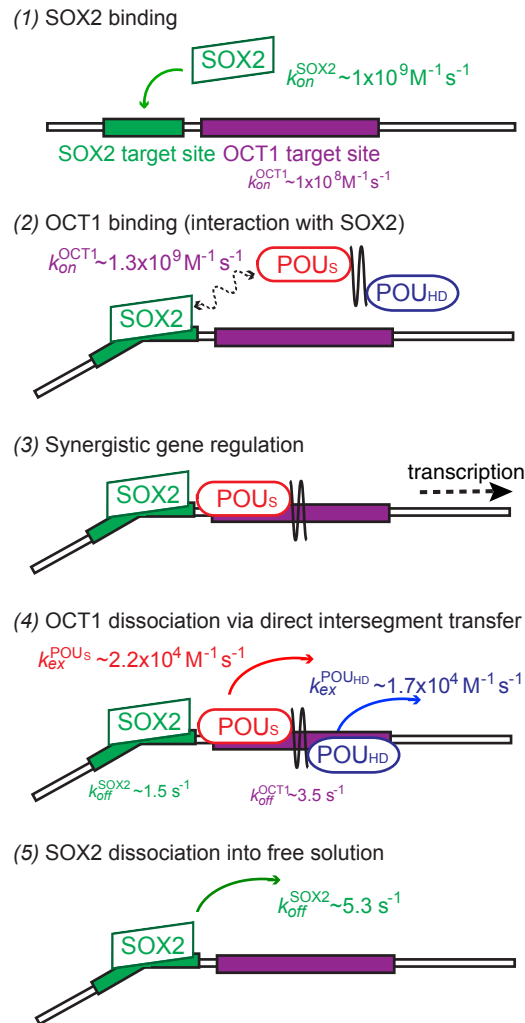


Figure 5 Model for the sequence of binding, intersegment transfer, and dissociation events involved in synergistic transcription regulation by SOX2 and OCT1 derived from z-exchange data on the SOX2:OCT1-*Fgf4*-DNA complex. Adapted from Takayama and Clore (2012a).

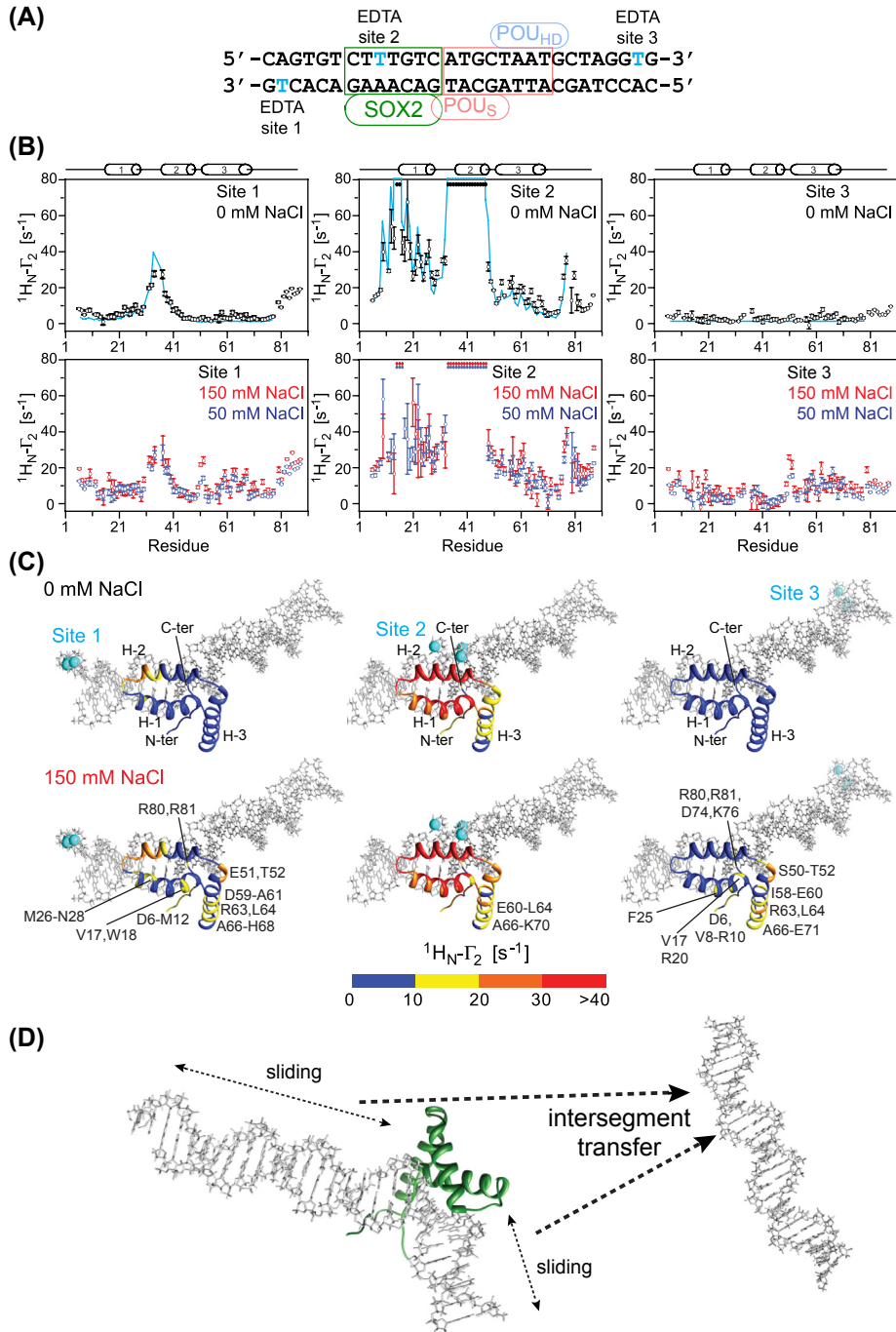
found in both the cytoplasm and the nucleus. The presence of specifically bound SOX2 accelerates the binding of OCT1 to its target site adjacent to that of SOX2 by just over an order of magnitude, and the ternary complex is stabilized by protein–protein interactions between SOX2 and the POU₅ domain of OCT1. Once the specific ternary complex is formed, OCT1 and SOX2 activate transcription synergistically. OCT1 subsequently dissociates from the ternary complex largely by direct intersegment transfer, which, at high concentrations of DNA found in vivo, is significantly faster than dissociation into free solution. Intersegment transfer can occur to another specific site on a different promoter or to a nonspecific site. These sites may be located on different DNA molecules or at a separation of greater than about 150bp on the same DNA, allowing transfer to occur via DNA looping. Finally, SOX2 dissociates slowly from its specific site and can subsequently re-associate to other specific or nonspecific sites.

INTERPLAY BETWEEN SOX2 AND OCT1 IN TRANSLOCATION INVOLVING SPARSELY POPULATED STATES PROBED BY PRE

Short-Lived Intermediates in Translocation of SOX2 from the Specific SOX2 DNA Binary Complex

Using a 29-bp DNA duplex with paramagnetic tags at three sites (one at a time) (Takayama and Clore, 2012b) (Figure 6(A)) reveals that at low-added salt concentrations (0 M NaCl), the PRE profiles from sites 1 and 2, located just 5' to or within the SOX2 binding site but on the major groove, respectively, are consistent with the structure of the specific SOX2 DNA binary complex (Figure 6(B) and (C), top panels). However, the PRE profiles from site 3, located distally on the 3' end of the DNA binding site, reveal the presence of small ($<7\text{ s}^{-1}$) but significant PREs (Figure 6(B), top right panel). At higher salt concentrations (50 or 150 mM NaCl), additional PREs within helix 3 are

Figure 6 PRE detection of sparsely populated intermediate states involved in specific DNA target site location by SOX2 (A) 29mer *Hoxb1*-DNA duplex used with the three sites (one at a time) paramagnetically labeled with EDTA-Mn²⁺ indicated in blue. The binding sites for SOX2 and OCT1 are indicated. (B) PRE profiles observed on ¹⁵N/²H-labeled SOX2 (in the absence of OCT1) originating from the three sites in the presence of 0 (top panels) or 50 and 150 mM (bottom panels) added NaCl. The blue lines in the top panels are the PREs back-calculated from the structure of the specific SOX2–DNA complex (Murphy et al., 2001). (C) PRE profiles at 0 (top) or 150 mM (bottom) added NaCl mapped onto the structure of the specific SOX2–DNA complex. The color scale for the PREs is shown at the bottom of the figure. (D) Schematic of intermolecular and intramolecular translocation pathways involving SOX2 bound specifically to DNA, as deduced from PRE measurements involving mixtures of specific and nonspecific DNA duplexes. The major translocation pathway involves intermolecular translocation initiated by sliding from the specific site to an immediately adjacent nonspecific site, followed by direct intersegment transfer to the nonspecific DNA duplex and then back to the specific DNA duplex. Adapted from Takayama and Clore (2012b).



observed from site 1 and all PREs from site 3 are increased in magnitude (Figure 6(B) and (C), bottom panels), although the ^1H - ^{15}N correlation spectrum remains unchanged and represents that of the specific complex (Takayama and Clore, 2012b). These PRE data are a direct reflection of sparsely populated (<1%) transient states that come into close proximity of the paramagnetic label. The use of samples comprising an equimixture of specific and nonspecific DNA, in which the paramagnetic label is attached to either the nonspecific (intermolecular translocation only) or specific (contributions from intramolecular and intermolecular translocation) DNA duplexes indicates that the PREs are largely caused by intermolecular translocation with a small (about 20%) contribution from sliding (Takayama and Clore, 2012b) (Figure 6(D)). Given the slow dissociation of the specific SOX2·DNA complex (see Section The Binary SOX2·DNA Complex), intermolecular translocation of SOX2, once bound to its specific target site, must occur by SOX2 sliding out of the specific site to make a nonspecific interaction with the DNA, followed by intersegment transfer between nonspecific sites located on different DNA molecules (Takayama and Clore, 2012b).

Short-Lived Intermediates in Translocation of SOX2 and OCT1 from the Specific SOX2·OCT1·*Hoxb1*-DNA Complex

One can use the same 29-bp DNA duplex used to study the binary SOX2·DNA complex to examine the impact of protein–protein interactions on the sampling of sparsely populated states of SOX2 and OCT1 within the context of the specific SOX2·OCT1·*Hoxb1*-DNA complex (The OCT1 binding site is immediately 3' of the SOX2 site (Figure 6(A)). For both SOX2 and OCT1 the presence of short-lived transient states, populated below 1%, is detected by PRE, especially at higher salt concentrations (50–150 mM NaCl) (Takayama and Clore, 2012b).

For SOX2, these PREs arise entirely from intermolecular translocation because no measurable intramolecular PRE contributions can be detected (Figure 7(A)). But just as in the case of the SOX2·DNA binary complex, this must first involve sliding to a nonspecific site immediately adjacent to the specific one because dissociation of SOX2 from its specific site is so slow (Takayama and Clore, 2012b).

In the case of OCT1, analysis of the PRE data indicates that the POU_S domain is largely fixed to its specific site through interaction with SOX2 (Figure 7(B)) (Takayama and Clore, 2012b), in direct contrast to the situation with the specific OCT1 DNA complex in which the POU_S domain largely directs intermolecular translocation (Takayama and Clore, 2011). For the POU_{HD} domain, however, the PRE data indicate that translocation in the context of the SOX2·OCT1·*Hoxb1*-DNA ternary complex is primarily intermolecular with some contribution from intramolecular translocation (Takayama and Clore, 2012b), in contrast to the situation in the binary OCT1·DNA complex in which intramolecular translocation predominates (Takayama and Clore, 2011). Furthermore, the intramolecular translocation of POU_{HD} to nonspecific sites on the 5'-side of the SOX2-specific site likely

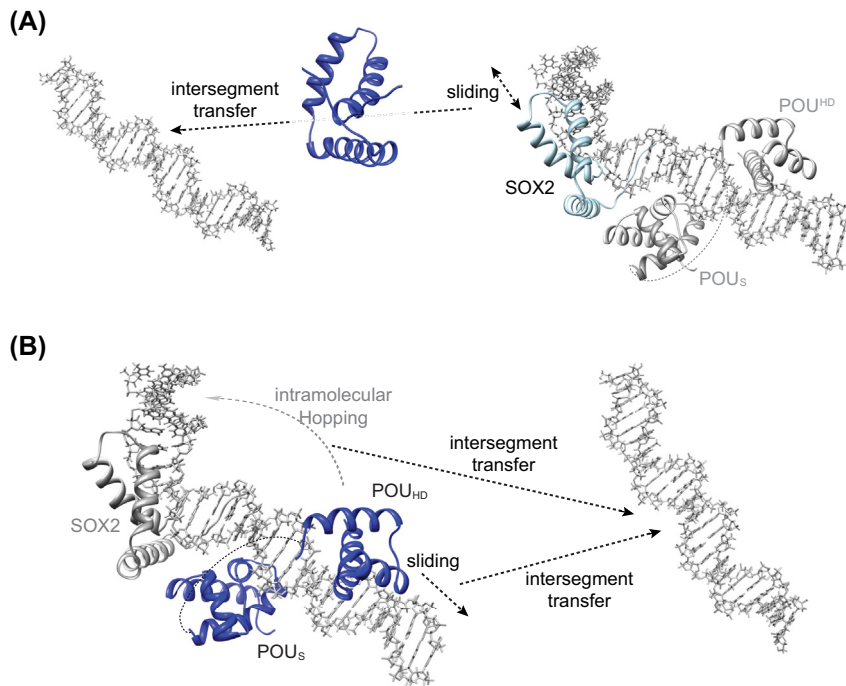


Figure 7 Schematic of intermolecular and intramolecular translocation pathways for (A) SOX2 and (B) OCT1 in the context of the specific ternary SOX2-OCT1-*Hoxb1*-DNA complex, derived from PRE measurements involving mixtures of specific and nonspecific DNA duplexes. Adapted from [Takayama and Clore \(2012b\)](#).

occurs via hopping rather than sliding because the presence of both SOX2 and the POU_S domain would block sliding of the POU^{HD} domain ([Figure 7\(B\)](#)).

CONCLUDING REMARKS

Data afforded by various NMR experiments including $^{15}\text{N}_z$ -exchange, line-width analysis, and PRE show that SOX2 efficiently explores the DNA landscape to locate its specific target site using both direct intersegment transfer between nonspecific sites on different DNA duplexes and sliding along the nonspecific DNA ([Takayama and Clore, 2012a,b](#)). Once a specific ternary SOX2-OCT1-DNA complex is formed, further sampling of DNA sites by SOX2 is reduced but can still occur by initial sliding of SOX2 to an adjacent nonspecific site followed by intersegment transfer. OCT1 alone explores the DNA landscape by using the complementary interplay of intramolecular sliding by the POU^{HD} domain and intersegment transfer of the POU_S domain, with the latter acting as a fly cast. Once the ternary complex with SOX2 is formed, the POU_S domain is largely fixed to its specific sites through protein-protein interactions with SOX2 which

are significantly stronger in the case of the complex on the *HOXB1* promoter than the *FGF4* enhancer owing to the shorter distance between the SOX2 and OCT1 sites (immediately adjacent versus separated by 3 bp, resulting in a twofold reduction for the latter in the buried accessible surface area at the interface between SOX2 and OCT1 (Williams et al., 2004; Remenyi et al., 2003)). However, the POU_{HD} domain can still sample other DNA sites by initially sliding to an immediately adjacent nonspecific site, just like SOX2, followed by either intersegment transfer to another DNA duplex or directly hopping to another nonspecific site on the same DNA molecule. The former involves the formation of a bridged intermediate complex in which POU_S and SOX2 are located on the first DNA duplex while POU_{HD} is transiently bound to the second DNA duplex, thereby promoting the complete release of OCT1 from the ternary complex by a first-order process involving dissociation of POU_S from the first DNA duplex followed by subsequent association onto the second DNA duplex. This contrasts to the mechanism used in the specific OCT1·DNA binary complex in which POU_S locates the second DNA duplex by intersegment transfer, thereby promoting the subsequent transfer of POU_{HD}. Thus, direct interaction of SOX2 and OCT1 bound to adjacent specific DNA binding sites modulates the translocation pathways employed by OCT1 to scan alternative DNA target sites via transient, sparsely populated states.

ACKNOWLEDGMENTS

This work was supported by the Intramural Program of the National Institute of Diabetes and Digestive and Kidney Diseases, National Institutes of Health and by the AIDS Targeted Antiviral Program of the Office of the Director of the National Institutes of Health.

REFERENCES

- Clore, G.M., 2011a. Exploring sparsely populated states of macromolecules by diamagnetic and paramagnetic NMR relaxation. *Protein Sci.* 20, 229–246.
- Clore, G.M., 2011b. Exploring translocation of proteins on DNA by NMR. *J. Biomol. NMR* 51, 209–219.
- Clore, G.M., Iwahara, J., 2009. Theory, practice, and applications of paramagnetic relaxation enhancement for the characterization of transient low-population states of biological macromolecules and their complexes. *Chem. Rev.* 109, 4108–4139.
- Dailey, L., Basilico, C., 2001. Coevolution of HMG domains and homeodomains and the generation of transcriptional regulation by Sox/POU complexes. *J. Cell. Physiol.* 186, 315–328.
- Douclevé, M., Clore, G.M., 2008. Global jumping and domain-specific intersegment transfer between DNA cognate sites of the multidomain transcription factor Oct-1. *Proc. Natl. Acad. Sci. U.S.A.* 105, 13871–13876.
- Iwahara, J., Anderson, D.E., Murphy, E.C., Clore, G.M., 2003. EDTA-derivatized deoxythymidine as a tool for rapid determination of protein binding polarity to DNA by intermolecular paramagnetic relaxation enhancement. *J. Am. Chem. Soc.* 125, 6634–6635.
- Iwahara, J., Clore, G.M., 2006a. Detecting transient intermediates in macromolecular binding by paramagnetic NMR. *Nature* 440, 1227–1230.
- Iwahara, J., Clore, G.M., 2006b. Direct observation of enhanced translocation of a homeodomain between DNA cognate sites by NMR exchange spectroscopy. *J. Am. Chem. Soc.* 128, 404–405.

- Iwahara, J., Schwieters, C.D., Clore, G.M., 2004. Characterization of nonspecific protein-DNA interactions by ^1H paramagnetic relaxation enhancement. *J. Am. Chem. Soc.* 126, 12800–12808.
- Iwahara, J., Zweckstetter, M., Clore, G.M., 2006. NMR structural and kinetic characterization of a homeodomain diffusing and hopping on nonspecific DNA. *Proc. Natl. Acad. Sci. U.S.A.* 103, 15062–15067.
- Kamachi, Y., Uchikawa, M., Kondoh, H., 2000. Pairing SOX off: with partners in the regulation of embryonic development. *Trends Genet.* 16, 182–187.
- McConnell, H.M., 1958. Reaction rates by nuclear magnetic resonance. *J. Chem. Phys.* 28, 430–431.
- Murphy, E.C., Zhurkin, V.B., Louis, J.M., Cornilescu, G., Clore, G.M., 2001. Structural basis for SRY-dependent 46-X,Y sex reversal: modulation of DNA bending by a naturally occurring point mutation. *J. Mol. Biol.* 312, 481–499.
- Remenyi, A., Lins, K., Nissen, L.J., Reinbold, R., Scholer, H.R., Wilmanns, M., 2003. Crystal structure of a POU/HMG/DNA ternary complex suggests differential assembly of Oct4 and SOX2 on two enhancers. *Genes Dev.* 17, 2048–2059.
- Sahu, D., Clore, G.M., Iwahara, J., 2007. TROSY-based z -exchange spectroscopy: application to the determination of the activation energy for intermolecular protein translocation between specific sites on different DNA molecules. *J. Am. Chem. Soc.* 129, 13232–13237.
- Takayama, Y., Clore, G.M., 2011. Intra- and intermolecular translocation of the bi-domain transcription factor OCT1 characterized by liquid crystal and paramagnetic NMR. *Proc. Natl. Acad. Sci. U.S.A.* 108, E169–E176.
- Takayama, Y., Clore, G.M., 2012a. Impact of protein/protein interactions on global intermolecular translocation rates of the transcription factors SOX2 and OCT1 between DNA cognate sites analyzed by z -exchange NMR spectroscopy. *J. Biol. Chem.* 287, 26962–26970.
- Takayama, Y., Clore, G.M., 2012b. Interplay between minor and major groove-binding transcription factors SOX2 and OCT1 in translocation on DNA studied by paramagnetic and diamagnetic NMR. *J. Biol. Chem.* 287, 14349–14363.
- Williams Jr., D.C., Cai, M., Clore, G.M., 2004. Molecular basis for synergistic transcriptional activation by OCT1 and SOX2 revealed from the solution structure of the 42-kDa OCT1.SOX2.*Hoxb1*-DNA ternary transcription factor complex. *J. Biol. Chem.* 279, 1449–1457.
- Wolberger, C., 1999. Multiprotein-DNA complexes in transcriptional regulation. *Annu. Rev. Biophys. Biomol. Struct.* 28, 29–56.